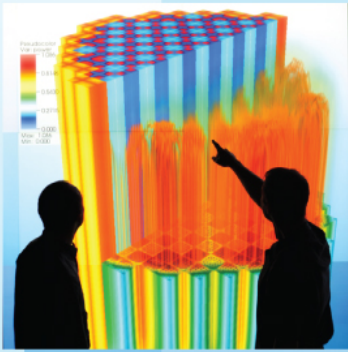


Power uprates  
and plant life extension



Engineering design  
and analysis



# Modeling and Analysis of Interfacial Heat transfer Phenomena in Subcooled Boiling Along PWR Coolant Channels

Rensselaer Polytechnic Institute

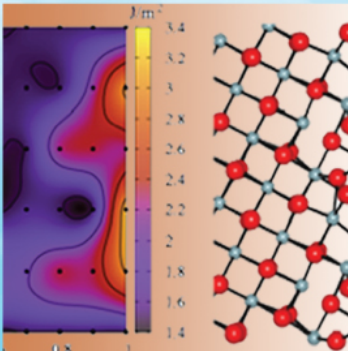
D. Shaver, S. Antal and M. Podowski

May 12-17, 2013:

Science-enabling  
high performance  
computing



Fundamental science



Plant operational data



U.S. DEPARTMENT OF  
**ENERGY**

**Nuclear Energy**

## MODELING AND ANALYSIS OF INTERFACIAL HEAT TRANSFER PHENOMENA IN SUBCOOLED BOILING ALONG PWR COOLANT CHANNELS

**Dillon R. Shaver, Steven P. Antal, and Michael Z. Podowski\***  
Center for Multiphase Research, Rensselaer Polytechnic Institute, USA

[shaved@rpi.edu](mailto:shaved@rpi.edu), [antals@rpi.edu](mailto:antals@rpi.edu), [podowm@rpi.edu](mailto:podowm@rpi.edu)\*

\*corresponding author

### ABSTRACT

The problem of subcooled boiling represents a significant challenge in nuclear reactor thermal hydraulics. The difficulties associated with accurate predictions of subcooled boiling are augmented by the fact that the underlying phenomena of two-phase flow and non-equilibrium heat transfer with phase change are closely coupled together.

The purpose of this paper is to present recent results on the development, testing and validation of a mechanistic multidimensional model of subcooled boiling phenomena in heated channels. The emphasis in the present work has been on formulating a complete model of the combined local vapor generation near the heated wall and the simultaneously occurring condensation in contact with subcooled liquid which is still present very close to the wall as long as the bulk liquid subcooling is high. It is important to notice that the high gradients in the near-wall temperature and vapor concentration require that special precautions be taken to assure the combined physical consistency and numerical accuracy of the results of computer simulations.

The model formulation is based on the Reynolds averaged Navier-Stokes (RANS) type multifield modeling framework. In this approach, a complete set of conservation equations is used for each component of the dispersed bubbly two-phase flow. The modeled interfacial interactions include energy, mass, and momentum transfer. In particular, a new model has been developed to properly capture the mechanisms governing the coupled interfacial heat and mass transfer between the liquid and vapor fields during simultaneous boiling and condensation.

The new model has been implemented in the NPHASE-CMFD computer code. The results of testing the overall model are presented and the effects of individual phenomena are discussed. The results of model validation against experimental data are presented. The predictions using the proposed model are in good agreement with the results of measurements.

### 1. INTRODUCTION

The accurate modeling and prediction of subcooled boiling requires a strong understanding of the underlying phenomena and how they interact. The model presented in this paper capitalizes on the framework provided by Kurul and Podowski [1]. The novel aspects of the proposed approach include the development of a consistent modeling framework for the combined evaporation and condensation phenomena in heated channels at subcooled boiling conditions,

which relies on individual phenomenological models rather than on experimental correlations. Such an approach should provide a robust overall modeling concept which can be applied to a broad range of geometries and operating conditions.

## 2. MODEL DESCRIPTION

The proposed model consists of three primary components: interfacial momentum transfer, interfacial mass and energy transfer in the bulk flow, and the simultaneous near-wall evaporation and condensation phenomena. Coupling these three components together provides a complete, consistent model of subcooled boiling.

A brief description of the individual models is given below. The proposed models have been implemented in the NPHASE-CMFD code [2]. In the present work, a two-fluid approach combined with the  $k$ - $\epsilon$  turbulence model has been used. NPHASE-CMFD has the ability to solve the mass, momentum, and interfacial jump condition equations in a coupled or segregated manner. The coupled solver is generally found to be more robust for multiphase flows and was used for this work. However, the energy conservation and turbulent quantity transport equations are solved in a segregated manner using a Jacobi method.

### 2.1 Interfacial Momentum Transfer

The interfacial momentum transfer model consists of the: drag, virtual mass, turbulent dispersion and lift forces, and also includes terms for momentum transfer due to phase change.

The drag force is formulated as

$$\bar{F}_d = -\frac{3}{4} \frac{C_d}{D_b} \alpha_v \rho_l |\bar{u}_v - \bar{u}_l| (\bar{u}_v - \bar{u}_l) \quad (1)$$

where  $D_b$  is the bubble diameter and  $\alpha_v$  is the vapor volume fraction. The drag coefficient is a function of the local relative bubble Reynolds number

$$C_d = \frac{24}{\text{Re}_b} (1 + 0.092 \text{Re}_b^{0.78}) \quad (2)$$

$$\text{Re}_b = \frac{\rho_l |\bar{u}_v - \bar{u}_l| D_b}{\mu_l} \quad (3)$$

The virtual mass force is expressed as [3]

$$\bar{F}_{vm} = -C_{vm} \rho_l \alpha_v \left( \frac{D\bar{u}_v}{Dt} - \frac{D\bar{u}_l}{Dt} \right) \quad (4)$$

where the differential operator  $D\bar{u}_i / Dt$  represents the material or substantial derivative. The value for the virtual mass coefficient is given as 0.5.

The lift force is modeled as [3]

$$\bar{F}_L = -C_L \rho_l \alpha_v (\bar{u}_v - \bar{u}_l) \times (\bar{\nabla} \times \bar{u}_l) \quad (5)$$

and the turbulent dispersion force is formulated as [4]

$$\bar{F}_{TD} = -C_{TD} \rho_l \alpha_v \underline{\underline{\kappa}}_l \nabla \alpha_v \quad (6)$$

where  $\underline{\kappa}_j = \overline{(u'_{i,j} u'_{i,j})} \delta_{ij}$  for  $i, j=1, 2, 3$ , and  $\delta_{ij}$  is the Kronecker delta.

It should be noted that for two-phase flows along heated pipes and conduits, Eqs.(5) and (6) are valid as long as the distance from the conduit walls is larger than the bubble diameter, i.e. as long as bubble motion is not constrained by the reaction force of the rigid wall. This is consistent with recent modeling work of Jiao and Podowski [5]. The lift coefficient has been chosen as 0.03, which is also consistent with the formulation provided by Jiao and Podowski [5].

In addition to the effect of interfacial forces, additional momentum transfer in diabatic flow is due to mass exchange (evaporation and/or condensation) between the vapor and liquid components. The resultant force of fluid component  $i$  acting on fluid component  $j$  is accounted for by

$$F_{\Gamma,j} = \sum_{i \neq j}^I (\Gamma_{i-j} \bar{u}_i - \Gamma_{j-i} \bar{u}_j) \quad (7)$$

where  $\Gamma_{i-j}$  represents the volumetric rate of mass transfer from field- $i$  to field- $j$ . The overall kinematic model has been validated before [6] against the experimental data of Wang et al. [7].

## 2.2 Interfacial Heat and Mass Transfer

The interfacial heat and mass transfer component assumes that a liquid-vapor interface is present at the saturation temperature. This applies to bubbles which have fully departed from the wall and got dispersed throughout the fluid flow domain. Heat transfer between the interface and each the liquid and vapor bubbles is modeled independently according to

$$q_j''' = N''' A_s H_j (T_{sat} - T_j) \quad (8)$$

where  $N'''$  represents the bubble number density,  $A_s$  is the bubble surface area, and  $H_j$  is the interfacial heat transfer coefficient. The subscript  $j$  indicates the individual fluid component, i.e. liquid or vapor. The condensation heat transfer coefficient (interface-to-liquid) is expressed as a function of the bubble relative Reynolds number [8]

$$Nu = C_{vol} \left[ 2 + (0.4 Re_b^{0.5} + 0.06 Re_b^{0.66}) Pr_l^{0.4} \right] = \frac{H_l D_b}{k_l} \quad (9)$$

The expression given with  $C_{vol} = 1$  was originally developed to model heat transfer to a single sphere. For bubbly two-phase flows, the value of  $C_{vol}$  is normally greater than one due an enhancement of heat transfer caused by bubble-induced turbulence.

In addition to the heat transfer on the liquid side of the interface, the present model also accounts for heat transfer inside the bubbles (important if bubbles contain superheated vapor). Since the corresponding mechanism is predominantly heat conduction, the approach is based on a rigorous solution to transient conduction in a sphere [9]. The rate of mass transfer is then determined by

$$\Gamma_{v-l} h_{fg} = q_l''' + q_v''' \quad (10)$$

where  $q_v'''$  is negative for superheated vapor. Extensive testing of the interfacial heat and mass transfer models for various vapor superheats and liquid subcoolings has been performed before [6].

### 2.3 Vapor Generation

A comprehensive model of wall heat flux partitioning in forced-convection boiling was originally proposed by Kurul and Podowski [1]. However the model was limited to subcooled boiling. To account for transition from subcooled to saturated boiling, a new approach has been developed and implemented in the current overall model.

In the new proposed model, the wall heat flux has been partitioned into two major components

$$q_w'' = q_b'' + q_{1\phi}'' \quad (11)$$

where  $q_{1\phi}''$  is the non-boiling (single-phase) component and  $q_b''$  is the boiling component which accounts for both evaporation and quenching. The single phase and boiling heat flux components are respectively given by

$$q_{1\phi} = H_{1\phi}(1 - A_b'')(\Delta T_w - \Delta T_l) \quad (12)$$

$$q_b'' = A_b'' \frac{h_{fg}}{h_g} q_w'' \quad (13)$$

and the fraction of heater's area exposed to boiling is determined from [10]

$$A_b'' = \left( \frac{\Delta T_w - \Delta T_0}{\Delta T_{nucl} - \Delta T_0} \right)^2 \quad (14)$$

where  $\Delta T_w$  is the wall superheat,  $\Delta T_0$  is the minimum wall superheat required for nucleation, and  $\Delta T_{nucl}$  is the wall superheat in well-established (saturated) nucleate boiling.

The current model provides a consistent solution for the wall temperature throughout the subcooled region and into the saturated boiling region. Its form allows for the investigation of individual phenomena associated with vapor generation.

In addition to the direct vapor generation model, a separate model of vapor condensation on the wall is included in the overall model. "Standing" bubbles which are formed at high subcooling but condense before they are able to depart from the wall are accounted for by this model. This allows boiling heat transfer to begin cooling the wall while there is practically no net generation of vapor, as observed in experiments [11, 12]. The model assumes that the heat transfer to a single "standing" bubble can be modeled as

$$q_0 = A_b H_{w,cond} \Delta T_l \quad (15)$$

where the wall-condensation heat transfer coefficient is calculated from Eq. (9), with the necessary adjustments associated with the neat-wall conditions. For example, the Reynolds number for a bubble on the wall is determined assuming the vapor phase has zero velocity, i.e. bubbles are attached to the wall

$$Re_{b,w} = \frac{\rho_l |\bar{u}_l| D_b}{\mu_l} \quad (16)$$

The wall condensation rate is be characterized by the condensation number, which represents the ratio of the heat transfer due to condensation to the maximum achievable heat transfer from condensation of all available vapor

$$Co = \frac{6H_{w,cond}(T_{sat} - T_l)}{D_b \rho_v f h_{fg}} \leq 1 \quad (17)$$

where  $f$  is the ebullition frequency. The wall condensation rate is then given by

$$\Gamma_{w,v-l} = Co \Gamma_{w,l-v} \quad (18)$$

By formulating the condensation model in this manner, the nucleation site density is implicitly determined from the boiling rate, rather than from a correlation. This provides a physically consistent formulation.

### 3. NUMERICAL IMPLEMENTATION

This model has been implemented in the state-of-the-art NPHASE-CMFD computer code [2], which independently solves conservation of mass, momentum and energy equations for any given number of fluid components (fields), along with turbulent quantities ( $k$  and  $\epsilon$ ) for the continuous field. The conservation of energy equation used for each fluid component in the NPHASE-CMFD code is given by [2]

$$\frac{\partial}{\partial t}(\alpha_j \rho_j h_j) + \nabla \cdot (\alpha_j \rho_j \bar{u}_j h_j) = \nabla \cdot [\alpha_j (\bar{q}_j'' + \bar{q}_{j,turb}'')] + \sum_{i \neq j} (\Gamma_{i-j} h_i - \Gamma_{j-i} h_j) + S_j''' \quad (19)$$

where the subscripts  $i$  and  $j$  indicate the individual fluid component fields and  $S_j'''$  represents a general source term that can be used to model interfacial heat transfer. Note that certain terms are negligible and are not included in the present formulation (e.g. viscous dissipation).

#### 3.1 Interfacial Heat and Mass Transfer

The proposed interfacial heat and mass transfer model is capable of accounting for both subcooled liquid and superheated vapor. In order to model interfacial condensation, the desired form of the energy equations for the liquid and vapor fields respectively is given by

$$\frac{\partial}{\partial t}(\alpha_l \rho_l h_l) + \nabla \cdot (\alpha_l \rho_l \bar{u}_l h_l) = \nabla \cdot [\alpha_l (\bar{q}_l'' + \bar{q}_{l,turb}'')] + \Gamma_{v-l} h_f + q_l''' \quad (20)$$

$$\frac{\partial}{\partial t}(\alpha_v \rho_v h_v) + \nabla \cdot (\alpha_v \rho_v \bar{u}_v h_v) = -\Gamma_{v-l} h_g + q_v''' \quad (21)$$

On the other hand, the NPHASE-CMFD formulation is

$$\frac{\partial}{\partial t}(\alpha_l \rho_l h_l) + \nabla \cdot (\alpha_l \rho_l \bar{u}_l h_l) = \nabla \cdot [\alpha_l (\bar{q}_l'' + \bar{q}_{l,turb}'')] + \Gamma_{v-l} h_v + S_l''' \quad (22)$$

$$\frac{\partial}{\partial t}(\alpha_v \rho_v h_v) + \nabla \cdot (\alpha_v \rho_v \bar{u}_v h_v) = -\Gamma_{v-l} h_v + S_v''' \quad (23)$$

Note that the diffusion term is not included in the vapor energy equation, since direct heat transfer does not occur between dispersed bubbles. Two energy source terms are used for each fluid component, one representing the energy associated with adding or removing mass from a field and the other representing sensible heat transfer. The default behavior is to have the source term associated with mass transfer carry the enthalpy of the donor field. Therefore, the source

term in NPHASE-CMFD must be adjusted to ensure that mass is generated or removed at the proper enthalpy. Specifically, we write

$$S_l''' = \Gamma_{v-l} (h_f - h_v) + q_l''' \quad (24)$$

$$S_v''' = \Gamma_{v-l} (h_v - h_g) + q_v''' \quad (25)$$

The gamma terms in these two equations can then be interpreted as a correction for superheated vapor. For the case of saturated vapor, it can be shown using Eqs.(8) and (10) that the volumetric heat sources in the energy equations become

$$q_l''' = \Gamma_{v-l} h_{fg} \quad (26)$$

$$q_v''' = 0 \quad (27)$$

and the source terms used in the NPHASE-CMFD formulation convert to

$$S_l''' = \Gamma_{v-l} (h_g - h_v) \quad (28)$$

$$S_v''' = \Gamma_{v-l} (h_v - h_g) \quad (29)$$

Then, the NPHASE-CMFD form of the energy conservation equations becomes

$$\frac{\partial}{\partial t} (\alpha_l \rho_l h_l) + \nabla \cdot (\alpha_l \rho_l \bar{u}_l h_l) = \nabla \cdot [\alpha_l (\bar{q}_l'' + \bar{q}_{l,turb}'')] + \Gamma_{v-l} h_g \quad (160)$$

$$\frac{\partial}{\partial t} (\alpha_v \rho_v h_v) + \nabla \cdot (\alpha_v \rho_v \bar{u}_v h_v) = -\Gamma_{v-l} h_g \quad (171)$$

which is consistent with the corresponding theoretical formulation.

### 3.2 Vapor Generation

The treatment of the vapor generation models is much more straightforward since the quenching heat transfer (i.e. the heat required to increase the liquid enthalpy to saturation) can be handled explicitly as

$$\Gamma_{l-v,w} h_{lg} = q_b''' \quad (182)$$

where  $h_{lg}$  represents the enthalpy difference between the local (possibly subcooled) liquid and saturated vapor. The desired forms of the energy equations are then given by

$$\frac{\partial}{\partial t} (\alpha_l \rho_l h_l) + \nabla \cdot (\alpha_l \rho_l \bar{u}_l h_l) = \nabla \cdot [\alpha_l (\bar{q}_l'' + \bar{q}_{l,turb}'')] - \Gamma_{l-v,w} h_l + \Gamma_{v-l,w} h_v + q_{l\phi}''' \quad (193)$$

$$\frac{\partial}{\partial t} (\alpha_v \rho_v h_v) + \nabla \cdot (\alpha_v \rho_v \bar{u}_v h_v) = \Gamma_{l-v,w} h_l - \Gamma_{v-l,w} h_v + q_b''' \quad (204)$$

Note that the volumetric single phase and boiling heat transfer terms must be properly translated using the local wall area and nodal volume. It is apparent that no correction terms are required for this model and the source terms in NPHASE-CMFD become

$$S_l''' = q_{l\phi}''' = q_{l\phi}'' \frac{A_w^{cell}}{V_w^{cell}} \quad (215)$$

$$S_v''' = q_b''' = q_b'' \frac{A_w^{cell}}{V_w^{cell}} \quad (226)$$

Since vapor generation determined in this manner is purely a wall effect, the associated terms in the energy equations are only active in the near-wall nodes, whereas the interfacial heat and mass transfer terms are active throughout the domain.

It is well known that liquid temperature experiences a steep drop in the near-wall region. In order to address this issue and to assure the independence of the calculated condensation rate of the computational mesh size, the reference liquid temperature,  $T_l$ , in Eq.(17) has been evaluated at a distance from the wall equal to  $\frac{3}{4}$  of bubble diameter. This provides a realistic average temperature the bubble surface is exposed to, while assuming that not all bubbles are fully grown when they begin condensing.

#### 4. RESULTS AND ANALYSIS

The results of NPHASE-CMFD predictions using the current model have been validated against the experimental results of Batolomei and Chanturia [11]. The presented case is for subcooled boiling of water at 4.5 MPa. The geometry is a cylindrical tube of 15.4 mm internal diameter and 2 m in length. A constant heat flux of 570 kW/m<sup>2</sup> is applied along the entire length and the inlet bulk liquid subcooling is 60 K. Fully-developed single-phase flow conditions are applied at the inlet. The simulation uses a constant bubble diameter of 0.75 mm and constant fluid properties. The chosen bubble size is consistent with model predictions based on the work of Memmel and Jensen [12]. The liquid properties are evaluated at the average subcooling, with the exception of density which is evaluated at saturation. Vapor properties are all evaluated at saturated conditions. As can be seen in Figure 1 and Figure 2, the agreement of the model predictions with the experimental data was quite good.

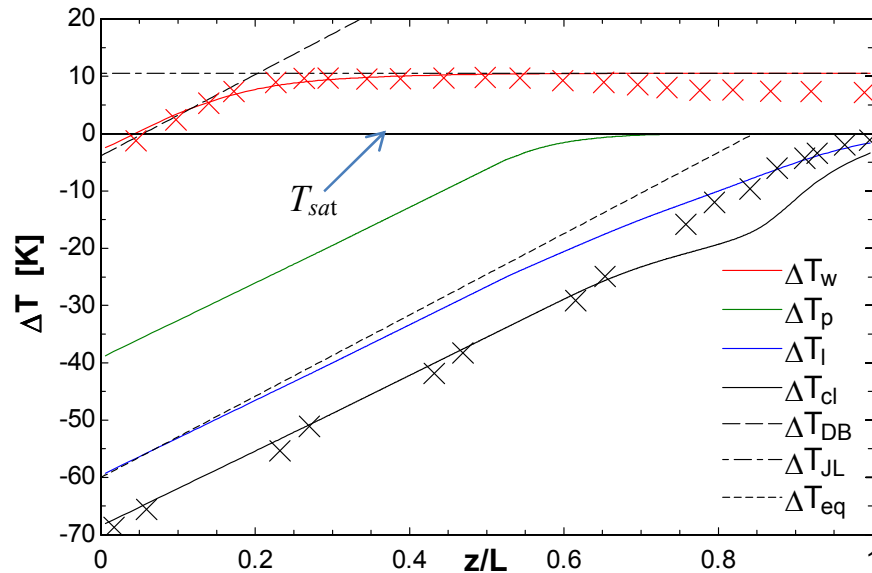


Figure 1. Axial temperature profiles predicted by NPHASE-CMFD (solid lines) compared to the experimental data (discrete points marked with X) of Bartolomei & Chanturia [11] with single phase and nucleate boiling correlations.

In particular, the model was capable of predicting the wall temperature in the first half of the channel length (before the onset of net generation of vapor). This is evident in Figure 1, which presents the calculated wall superheat,  $\Delta T_w$ , along with the near-wall temperature,  $\Delta T_p$ , the liquid bulk temperature,  $\Delta T_l$ , and liquid centerline temperature,  $\Delta T_{cl}$ . In addition, the Dittus-Boelter and Jens-Lottes correlations, and the calculated equilibrium temperature are presented for comparison. A difference shown in Figure 1 between the calculated and measured centerline temperatures for  $0.75 < z/L < 0.9$  has likely been caused by the fact that the effect of bubbles on turbulence enhancement in this region was slightly underestimated.

The channel averaged ( $\alpha_{ave}$ ) and near-wall ( $\alpha_p$ ) vapor volume fractions are presented in Figure 2. Agreement between the NPHASE- CMFD prediction and the experimentally measured average volume fraction is quite good. In addition, the results of extensive parametric test calculations have demonstrated the importance of the new near-wall condensation model. Indeed, without the wall condensation model, the onset of vapor generation would be predicted to occur much farther upstream, and an excessive amount of vapor would accumulate near the wall.

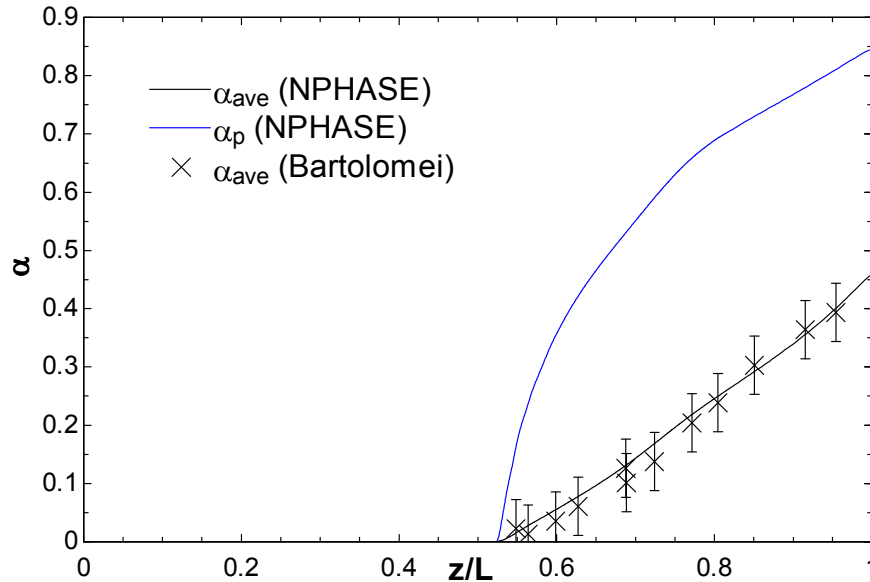


Figure 2. Average void fraction and near-wall void fraction as predicted by NPHASE-CMFD, both with the wall condensation model (solid lines) and without (dashed lines), compared to experimental data.

Contour plots of the predicted liquid subcooling, condensation rate, and vapor volume fraction are shown in Figure 3. This figure is oriented such that the heated wall is on the left and flow is in the upward direction with gravity downward. The highest condensation rates are observed along the wall where the flow is strongly subcooled. This corresponds to where the vapor is condensing on the wall before the onset of net production of vapor. Towards the outlet of the domain, the liquid approaches the saturation temperature and the condensation rate can be seen to decrease, even in areas with high vapor concentration. The multidimensional effects of the model are clearly demonstrated.

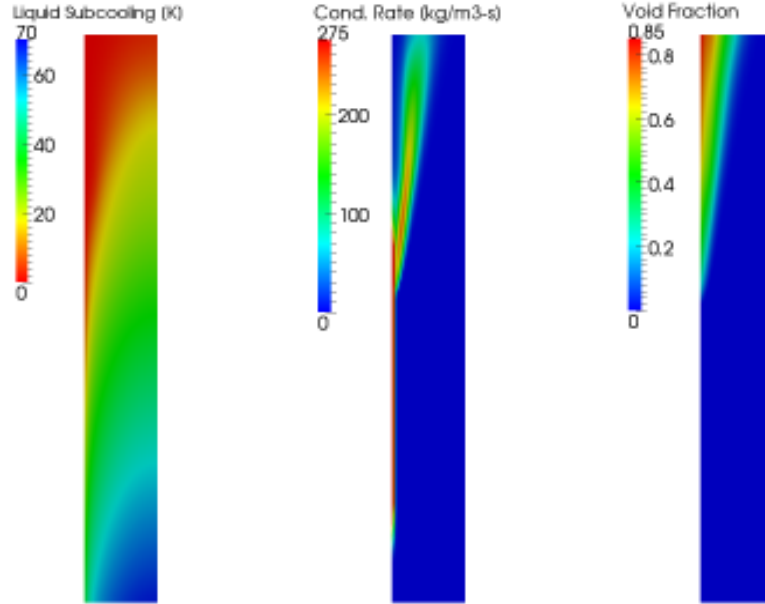


Figure 3. Contour plots of predicted vapor volume fraction, liquid subcooling and condensation rate. Note the aspect ratio has been skewed for graphical convenience.

The effects of the wall-condensation model are further illustrated in Figure 4, which shows the linear mass transfer rates for boiling, net condensation, wall condensation and interfacial (volumetric) condensation. In the region before the onset of net vapor generation, the wall condensation is observed to be equal to the wall boiling. This essentially causes the flow to behave like single-phase flow. However, since the model accounts for boiling, heat transfer from the wall is enhanced. Beyond this point, wall condensation quickly decreases due to the near-wall temperature approaching saturation whereas volumetric condensation increases due to the formation of vapor.

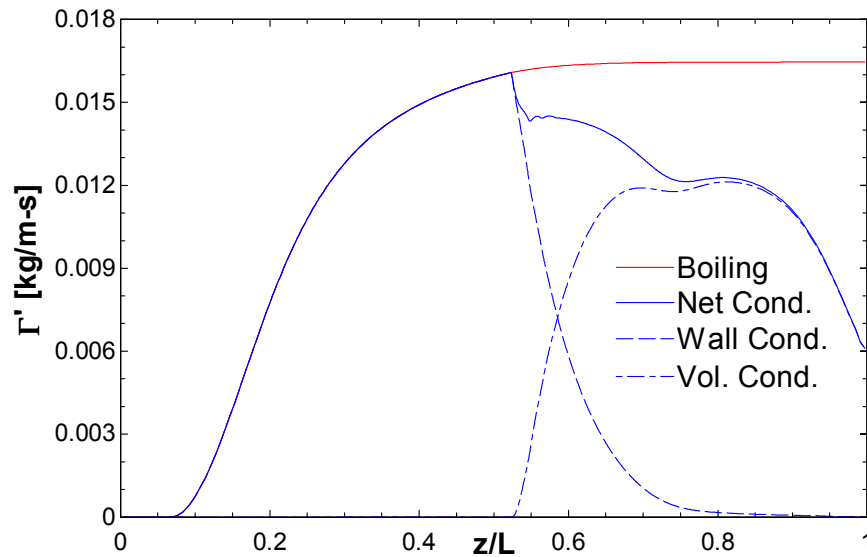


Figure 4. Rates of mass transfer for boiling and condensation models.

Radial liquid temperature profiles are presented in Figure 5 at various locations along the flow. Typical single-phase behavior is demonstrated in the first half of the channel, before the onset of net vapor generation. In the second half, the profiles are distorted. Two different phenomena affect the temperature profiles in this region. On the one hand, direct heating of the liquid from the wall is strongly diminished, while on the other hand, heating due to condensation of vapor is increased and is distributed across the radius of the channel.

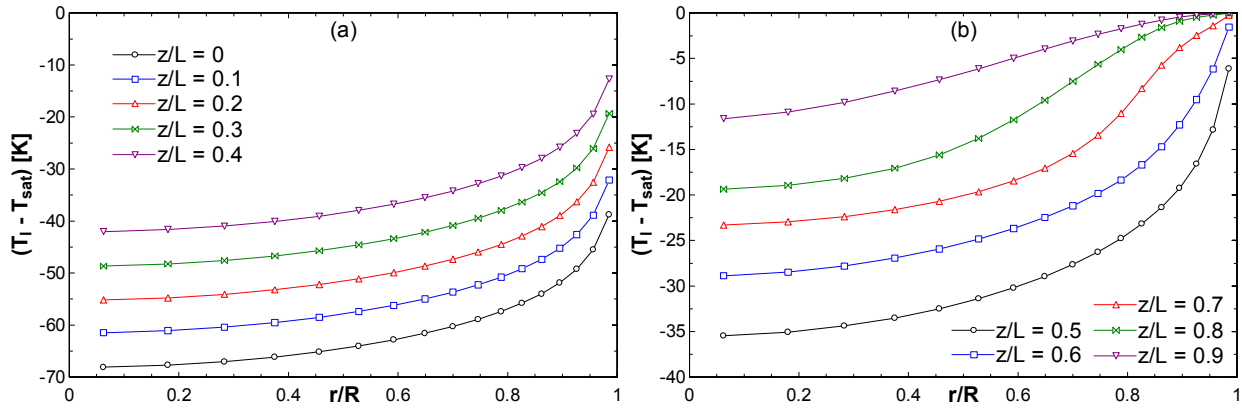


Figure 5. Liquid radial temperature profiles in (a) the first half of the channel and (b) the last half.

Condensation occurs where vapor is in contact with subcooled liquid. From Figure 3 it can be seen that this is most prevalent at the outer edge of the vapor penetration into the channel. The distribution of vapor across the channel is presented in Figure 6 for the outlet half of the channel.

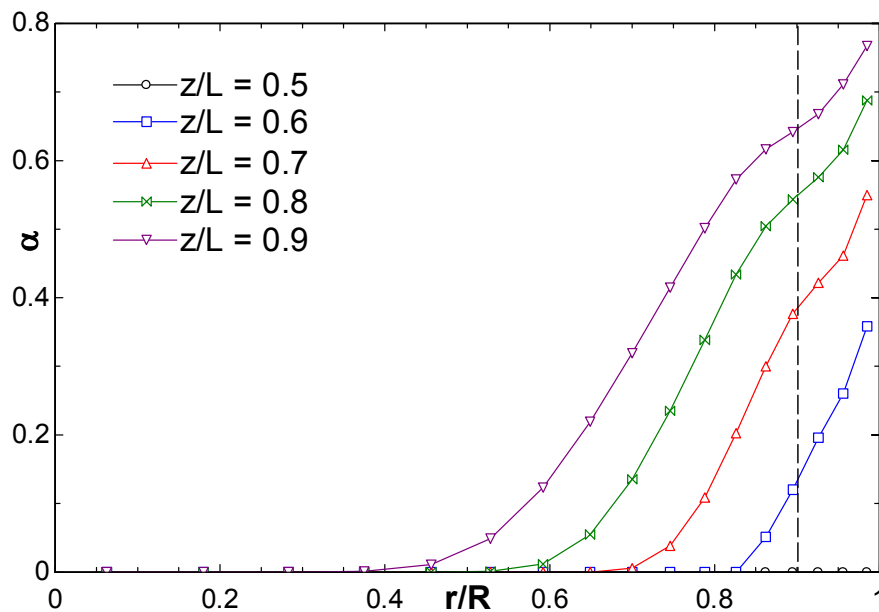


Figure 6. Radial void fraction profiles for the last half of the channel.

The vertical dashed line represents the distance from the wall equal to the bubble diameter. It should be noted that for the computational points nearer to the wall than this line, the interfacial momentum transfer model becomes inapplicable due to the reaction force caused by the presence of the wall. However, the overall trend is as expected, with the highest concentration near the wall, where vapor is formed, decreasing with the increasing distance from the wall. No vapor is predicted to penetrate deeper into the channel than  $r/R = 0.4$ . This is due to a high liquid subcooling still present in this region.

## 5. CONCLUSIONS AND FUTURE WORK

A model for predicting the heated wall temperature in subcooled boiling has been presented. The proposed model is able to isolate vapor generation from the details of the ebullition cycle, allowing for in-depth parametric testing. It has been shown that the model predictions are consistent with the underlying physical phenomena and selected experimental data. Also, the multidimensional effects of wall heating, phase distribution and interfacial heat transfer in subcooled boiling have been demonstrated. Furthermore, the predicted wall temperature and volume fraction are in good agreement with the experimental data of reference. It is interesting to mention that whereas the radial void distribution was not measured in the Bartolomei a& Chanturia [11] experiments, direct comparisons between predictions and data were performed in the past by Prof. Podowski and his collaborators [13]. Also, the radial void distribution predictions by the present model have already shown good agreement against experimental data for adiabatic gas/liquid flows [7].

Continued work will focus on further comparison of the model to experimental data, modeling improvements, and model application to prototypic geometries and operating conditions of typical PWRs.

## ACKNOWLEDGEMENTS

The authors would like to acknowledge the financial support provided to this study by the CASL Program of the U.S. Department of Energy.

## REFERENCES

1. N. Kurul and M. Z. Podowski, "On the Modeling of Multidimensional Effects in Boiling Channels", *ANS Proc. National Heat Trans. Conf.* (1991).
2. S.P. Antal, *NPHASE-CMFD User Manual*, Interphase Dynamics, LLC, (2011).
3. D.A. Drew and R.T. Lahey, Jr., "Application of General Constitutive Principles to the Derivation of Multidimensional Two-Phase Flow Equations", *Int. J Multiphase Flow*, vol. 7, 243-264, (1979).
4. M.Z. Podowski, "On the Consistency of Mechanistic Multidimensional Modeling of Gas/Liquid Two-Phase Flows", *Nucl. Eng. and Design*, 239, 933-934, (2009).
5. H Jiao and M.Z. Podowski, "An Analysis of Multidimensional Models of Gas/Liquid Flows", *Proc. Amer. Nucl. Soc. Winter Meeting*, vol. 107, 1393-1394, San Diego, CA, (2012).
6. D.R. Shaver, S.P. Antal and M.Z. Podowski, "Multidimensional Mechanistic Modeling of Interfacial Heat and Mass Transfer", *Proc. Int. Congress on Advances in Nuclear Power Plants (ICAPP'12)*, Chicago, IL, USA (2012).

7. S.K. Wang, S.J. Lee, O.C. Jones, and R.T. Lahey Jr., “3-D Turbulence Structure and Phase Distribution Measurements in Bubbly Two-Phase Flows”, *Int. J Multiphase Flow*, Vol. 13 No.3, (1987).
8. A. Bejan, *Convection Heat Transfer*, John Wiley and Sons Inc., Hoboken, NJ, (2007).
9. D.R. Shaver, S.P. Antal, M.Z. Podowski and D.H. Kim, “Direct Steam Condensation Modeling for a Passive PWR Safety System”, *Proc. CFD4NRS-3*, Washington, D.C., USA, (2010).
10. M.Z. Podowski, “Toward Mechanistic Modeling of Boiling Heat Transfer”, *Nuclear Engineering and Technology*, Vol.44, No.8, 2012.
11. G.G. Bartolomei and V.M. Chanturia, “Experimental Study of True Void Fraction when Boiling Subcooled Water in Vertical Tubes”, *Thermal Engineering*, Vol. 14., (1967).
12. M.K. Jensen and J.G.J. Memmel, 1986, Evaluation of Bubble Departure Diameter Correlations, *Proc. Eighth Int. Heat Transfer Conf.*, 4, pp.1907-1912.
13. A. Alajbegovic, N. Kurul, D.A. Drew, R.T. Lahey, Jr. and M.Z. Podowski, “A CFD Analysis of Multidimensional Phenomena in Two-Phase Flow Using a Two-Fluid Model”, *ANS Proc., 1996 National Heat Transfer Conference*, HTC-Vol. 9, 1996, pp. 387-396.